The 2009 IEEE/RSJ International Conference on
Intelligent Robots and Systems
October 11-15, 2009 St. Louis, USA

Impedance Control of Manipulators Carrying a Heavy Payload

Farhad Aghili

***Abstract*— A heavy payload attached to the wrist force/moment (F/M) sensor of a manipulator can fail the conventional impedance controller to establish a desired impedance due to the non-contact components of the force measurement, i.e., the inertial and gravitational forces of the payload. This paper proposes an impedance control scheme for such a manipulator to accurately shape its force-response without needing any acceleration measurement. Therefore, no wrist accelerometer or a dynamic estimator for compensating the load inertial forces are required. The impedance controller is further developed using an inner/outer loop feedback approach that allows not only to overcome the robot dynamics uncertainty, but also to specify the target impedance model in a general form, e.g., a nonlinear model. The stability and convergence of the impedance controller are analytically investigated, and the results show that that control input remains bounded provided that the desired inertia is selected to be different from the payload inertia. Experimental results demonstrate that the proposed impedance controller is able to accurately shape the impedance of a manipulator carrying a relatively heavy load according to a desired impedance model.**

I. INTRODUCTION

The impedance control of a manipulator to shape its force-response was proposed by Hogan [1]. In his approach the contact force, measured by a wrist force/torque sensor, is used by the controller to establish a relation between force and velocity according to the impedance model. Contact stability of the conventional impedance controllers has been analyzed [2], [3]. Lasky *et al.* [4] proposed the inner/outer loop control scheme for impedance control of manipulator to compensate the robot dynamics uncertainties by a position control algorithm in the inner loop, while adaptive impedance control schemes for robots with uncertain dynamic model parameters are presented in [5], [6]. The stability of impedance control in dealing with unknown environment has been addressed in [7]–[9]. All of above impedance control approaches suppose that the direct measurements of external or contact force/moment are available.

In the case that the manipulator carries a payload with significant inertia, the conventional impedance controller can fail to achieve the desired impedance, because, the measurement of the wrist force sensor have components of not only the external forces but also the inertial and gravitational forces of the payload [10]. In addition, a heavy payload can significantly change the manipulator dynamics. Particularly, space manipulators can handle very heavy payload owing to the weightlessness environment of the space; e.g., the Dexter manipulator of the International Space Station (ISS) can handle payloads as massive as 600 kg.

Approaches to deal with the non-contact force components of a manipulator wrist F/M sensor are mainly based on compensating for the inertial force components of the sensor measurements using one kind of estimator or another, rather than modifying the impedance control law itself. Estimation of inertial components of a force sensor signal for the case where the planned trajectories are known beforehand was addressed in [11]. Uchiyama *et al.* proposed an estimation method to extract the external forces and moments from the forces and moments measured by a force sensor [12]. Their method includes dynamic modeling of the process of force sensing and estimation of the external forces and moments by an extended Kalman filter. However, the convergence of extended Kalman filter is not guaranteed because that depends on the *persistent excitation* of the input signals [13], [14]. A method of eliminating all non-contact force components of the force sensor measurements by fusing force and accelerometer sensors in an extended Kalman filter was proposed in [15]. This estimation technique was further developed in [14] for estimating not only the inertial forces but also all ten inertial parameters of the load as well as the sensor offset. However, these estimation techniques require an additional 6-axis accelerometer sensor. Contrary to the above approaches, we do not use a dynamic estimator or an accelerometer to estimate the inertial forces of the load. Rather, the impedance control law per se is modified so that it can directly incorporate feedback signal from the force sensor to establish the desired impedance. From a practical point of view, the advantage of this approach is that one does not need to deal with the excitation of the input signal for convergence of a dynamic estimator or with the stability of the closed-loop system of the dynamic estimator and a force controller. Moreover, the additional 6-axis accelerometer device to be attached to the manipulator wrist is not required in the proposed method.

The purpose of this paper is to present an impedance control scheme for manipulators carrying a heavy payload that does not require compensating for the inertial components of the force/moment measurement. Investigating the limitations of such an impedance controller scheme is also aimed in this work. The impedance controller takes the force/moment measurements from a force-sensor installed between the manipulator wrist and its payload to establish the dynamic relation between force error and position error according to the standard mass-damping-spring model. The impedance controller is further developed using an inner/outer loop feedback approach that allows specifying the target impedance

F. Aghili is with the Spacecraft Engineering Division of the Space Technologies, Canadian Space Agency, Saint-Hubert, Quebec J3Y 8Y9, Canada farhad.aghili@space.gc.ca

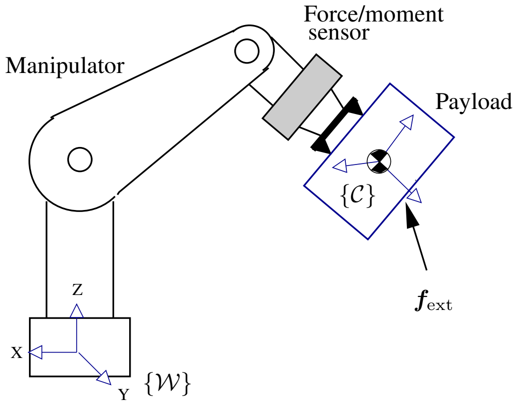

Fig. 1. A manipulator carrying a heavy payload.

model in a general form. Using the robust control theory [16], [17], we also show that the control algorithm can overcome the modeling uncertainty. Stability and convergence of the robot impedance to the target impedance under the proposed impedance control scheme have been analyzed.

This paper is organized as follows: Section II introduces the impedance control law for manipulators carrying a heavy payload. The impedance controller is further developed in Section III using an inner/outer control scheme. Finally, Section IV presents some experimental results.

II. Impedance Control

Fig. 1 shows a manipulator carrying a payload with non-negligible mass. Denote $\boldsymbol{q} \in \mathbb{R}^n$ as the vector of the manipulator joint angles. Without loss of generality, we assume that $n = 6$ and that no kinematic singularities are encountered meaning that the robot can always operate in the 6-dimensional task space. A 6-axis force/moment sensor installed at the manipulator wrist to measure the external force applied to the payload. However due to the payload mass, the force sensor signal $\boldsymbol{f}'_s$ contains the component of the generalized external force $\boldsymbol{f}'_{\text{ext}}$ superimposed by the gravitational and inertial forces of the payload. Let assume that vector $\boldsymbol{x}$ is the minimal representation of the position and orientation of the payload, $\boldsymbol{v}$ and $\boldsymbol{\omega}$ are the linear and angular velocities of the payload expressed in the fixed-body frame $\{\mathcal{C}\}$, and $\boldsymbol{\nu} = \operatorname{col}(\boldsymbol{v}, \boldsymbol{\omega})$ is the vector of *generalized velocity*. Then, the following mapping through the manipulator Jacobian matrix $\tilde{\boldsymbol{J}}(\boldsymbol{q})$ is in order

$$\boldsymbol{\nu} = \boldsymbol{L}(\boldsymbol{x})\dot{\boldsymbol{x}} = \boldsymbol{J}'(\boldsymbol{q})\dot{\boldsymbol{q}}, \tag{1}$$

where $\boldsymbol{L} = \operatorname{diag}(\boldsymbol{1}_3, \boldsymbol{L}_o)$ with $\boldsymbol{1}_3$ being the 3×3 identity matrix, and transformation matrix $\boldsymbol{L}_o$ depends on a particular set of parameters used to represent the orientation [18]. The above kinematic mapping can be also written as $\dot{\boldsymbol{x}} = \boldsymbol{J}(\boldsymbol{q})\dot{\boldsymbol{q}}$, where $\boldsymbol{J}(\boldsymbol{q}) = \boldsymbol{L}^{-1}\boldsymbol{J}'(\boldsymbol{q})$ is called the *analytical Jacobian* [18]; here we have assumed that no *representation singularities* of the rotation occurs. According to the *virtual work* principal, two sets of generalized forces $\boldsymbol{f}'$ and $\boldsymbol{f}$ performing work on $\boldsymbol{\nu}$ and $\dot{\boldsymbol{x}}$ satisfy $\boldsymbol{\nu}^T\boldsymbol{f}' = \dot{\boldsymbol{x}}^T\boldsymbol{f}$, and hence they are related by $\boldsymbol{f}_s = \boldsymbol{L}^T\boldsymbol{f}'_s$ and $\boldsymbol{f}_{\text{ext}} = \boldsymbol{L}^T\boldsymbol{f}'_{ext}$.

Now, assume that the manipulator is cut right at its junction to the payload. Note that the interaction force and moment between the two separated systems of the manipulator and the payload are detected by the force/moment sensor. Then, the equation of motion of the payload in the task space can be written by

$$\boldsymbol{M}_p\ddot{\boldsymbol{x}} + \boldsymbol{h}_p(\boldsymbol{q}, \dot{\boldsymbol{q}}) = -\boldsymbol{f}_s + \boldsymbol{f}_{\text{ext}}, \tag{2}$$

where

$$\boldsymbol{M}_p = \begin{bmatrix} m_p\boldsymbol{1}_3 & \boldsymbol{0} \\ \boldsymbol{0} & \boldsymbol{L}_o^T\boldsymbol{I}_p\boldsymbol{L}_o \end{bmatrix} \tag{3a}$$

$$\boldsymbol{h}_p = \begin{bmatrix} m_p\big(\boldsymbol{\omega} \times \boldsymbol{v} + g\boldsymbol{R}^T\boldsymbol{k}\big) \\ \boldsymbol{L}^T\big(\boldsymbol{\omega} \times \boldsymbol{I}_p\boldsymbol{\omega}\big) + \boldsymbol{L}^T\boldsymbol{I}_p\dot{\boldsymbol{L}}_o\boldsymbol{L}_o^{-1}\boldsymbol{\omega} \end{bmatrix}. \tag{3b}$$

Here, m_p and $\boldsymbol{I}_p$ are the payload mass and inertia tensor, rotation matrix $\boldsymbol{R}(\boldsymbol{q})$ represents the end-effector attitude, unit vector $\boldsymbol{k}$ is aligned with the gravity vector [1] which is expressed in the manipulator's base frame $\{W\}$, and $g = 9.81$ m/s^2. Note that all force terms in the right-hand-side (RHS) of (2) are expressed in the fixed-body coordinate frame $\{C\}$ whose origin coincides with the payload's center-of-mass. Note that the linear and angular velocities in (3b) can be computed from the manipulator's joint angles and velocities using the kinematic relation (1), and hence the nonlinear vector $\boldsymbol{h}_p$, which contains the Coriolis, centrifugal and gravitational terms associated with the payload, can be expressed as a function of the joint angles and velocities, i.e., $\boldsymbol{h}_p = \boldsymbol{h}_p(\boldsymbol{q}, \dot{\boldsymbol{q}})$.

It is known that the dynamics model of a manipulator in the task space becomes [18]

$$\boldsymbol{M}_m\ddot{\boldsymbol{x}} + \boldsymbol{h}_m(\boldsymbol{q}, \dot{\boldsymbol{q}}) = \boldsymbol{u} + \boldsymbol{f}_s, \tag{4}$$

where

$$\boldsymbol{u} = \boldsymbol{J}^{-T}\boldsymbol{\tau},$$

$\boldsymbol{M}_m$ is the Cartesian inertia matrix of the manipulator; nonlinear vector $\boldsymbol{h}_m(\boldsymbol{q}, \dot{\boldsymbol{q}})$ contains the Coriolis, centrifugal and gravitational terms; and $\boldsymbol{\tau}$ is the vector of joint torques (see Appendix I for details). Assuming kinematic singularity does not occur, there is an one-to-one correspondence with the joint vector $\boldsymbol{\tau}$ and auxiliary input $\boldsymbol{u}$. Therefore, in the following derivation, we will take $\boldsymbol{u}$ as the control input for the sake of simplicity. Now, eliminating the interaction force $\boldsymbol{f}_s$ from (2) and (4), we can express the combined dynamics of the manipulator and the payload by

$$\boldsymbol{M}_t(\boldsymbol{q})\ddot{\boldsymbol{x}} + \boldsymbol{h}_t(\boldsymbol{q}, \dot{\boldsymbol{q}}) = \boldsymbol{u} + \boldsymbol{f}_{\text{ext}}, \tag{5a}$$

where

$$\boldsymbol{M}_t = \boldsymbol{M}_p + \boldsymbol{M}_m, \tag{5b}$$

$$\boldsymbol{h}_t = \boldsymbol{h}_p + \boldsymbol{h}_m. \tag{5c}$$

The desired impedance model that dynamically balances the external contact force $\boldsymbol{f}_{\text{ext}}$ is typically chosen as the second-order system [18]

$$\boldsymbol{M}_d(\ddot{\boldsymbol{x}} - \ddot{\boldsymbol{x}}_d) + \boldsymbol{D}_d(\dot{\boldsymbol{x}} - \ddot{\boldsymbol{x}}_d) + \boldsymbol{K}_d(\boldsymbol{x} - \boldsymbol{x}_d) = \boldsymbol{f}_{\text{ext}}, \tag{6}$$

[1] If the z-axis of the coordinate frame $\{W\}$ is perfectly parallel to the earth's gravity vector, then $\boldsymbol{k} = \operatorname{col}(0, 0, -1)$.

where $\boldsymbol{M}_d$, $\boldsymbol{D}_d$ and $\boldsymbol{K}_d$ are the desired inertia, damping and stiffness, respectively. Eliminating the acceleration from (2) and (6) and then from (5a) and (6), we get a set of two equations as:

$$\begin{aligned}\boldsymbol{f}_{\text{ext}} &= (\mathbf{1} - \boldsymbol{M}_p\boldsymbol{M}_d^{-1})^{-1}\big(\boldsymbol{f}_s + \boldsymbol{h}_p + \boldsymbol{M}_p\ddot{\boldsymbol{x}}_d\big) \qquad (7a)\\ &+ \big(\mathbf{1} - \boldsymbol{M}_d\boldsymbol{M}_p^{-1}\big)^{-1}(\boldsymbol{D}_d\dot{\boldsymbol{e}} + \boldsymbol{K}_d\boldsymbol{e}),\\ \boldsymbol{u} &= \boldsymbol{M}_t\big(\ddot{\boldsymbol{x}}_d - \boldsymbol{M}_d^{-1}(\boldsymbol{D}_d\dot{\boldsymbol{e}} + \boldsymbol{K}_d\boldsymbol{e})\big) + \boldsymbol{h}_t \qquad (7b)\\ &+ (\boldsymbol{M}_t\boldsymbol{M}_d^{-1} - \mathbf{1})\boldsymbol{f}_{\text{ext}}\end{aligned}$$

where $\boldsymbol{e} = \boldsymbol{x} - \boldsymbol{x}_d$ is the position error. Finally, substituting $\boldsymbol{f}_{\text{ext}}$ from (7a) into (7b) we obtain the overall impedance control law as

$$\begin{aligned}\boldsymbol{u} &= \big(\boldsymbol{M}_t(\boldsymbol{q}) - \boldsymbol{\Gamma}(\boldsymbol{q})\boldsymbol{M}_p\big)\big(\ddot{\boldsymbol{x}}_d - \boldsymbol{M}_d^{-1}(\boldsymbol{D}_d\dot{\boldsymbol{e}} + \boldsymbol{K}_d\boldsymbol{e})\big)\\ &+ \boldsymbol{h}_t(\dot{\boldsymbol{q}}, \boldsymbol{q}) - \boldsymbol{\Gamma}(\boldsymbol{q})\big(\boldsymbol{f}_s + \boldsymbol{h}_p(\dot{\boldsymbol{q}}, \boldsymbol{q})\big) \qquad (8a)\end{aligned}$$

where

$$\boldsymbol{\Gamma}(\boldsymbol{q}) \triangleq \mathbf{1} - \boldsymbol{M}_m\boldsymbol{M}_d^{-1}\big(\mathbf{1} - \boldsymbol{M}_p\boldsymbol{M}_d^{-1}\big)^{-1}. \qquad (8b)$$

By inspection, one can show that the impedance control law (8) coincides with the conventional impedance control law [18] if $\boldsymbol{M}_p \equiv \mathbf{0}$.

From a stability point of view, the fundamental difference between impedance control of manipulators without and with a payload is that, unlike the former case, the latter does not always lead to a stable system. Denote

$$\boldsymbol{\Delta}_d \triangleq \boldsymbol{M}_p\boldsymbol{M}_d^{-1}. \qquad (9)$$

Then, it is apparent from expressions (8a) and (8b) that the control input remains bounded if matrix $\mathbf{1} - \boldsymbol{\Delta}_d$ is not singular, i.e.,

$$\det(\mathbf{1} - \boldsymbol{\Delta}_d) \neq 0. \qquad (10)$$

Since $\det(\mathbf{1} - \boldsymbol{\Delta}_d) = \prod_i(1 - \lambda_i(\boldsymbol{\Delta}_d))$, then we can sat that (10) is equivalent to

$$\lambda_i(\boldsymbol{\Delta}_d) \neq 1 \qquad \forall i = 1, \cdots, n. \qquad (11)$$

In the case that the desired inertia is a diagonal matrix with all of its diagonal elements equal to m_d, i.e., $\boldsymbol{M}_d = m_d\mathbf{1}_n$, the above condition is reduced to

$$m_d \neq \lambda_i(\boldsymbol{M}_p) \qquad \forall i = 1, \cdots, n. \qquad (12)$$

Theorem 1: Assume that the desired inertia matrix is selected such that (11) is satisfied. Then, applying control law (8a) to the manipulator system (4) attached to a payload with generalized inertia $\boldsymbol{M}_p$ establishes the desired impedance (6) between the external force $\boldsymbol{f}_{\text{ext}}$ and the position error.

III. Impedance Control with Inner/Outer Loop

In this section, we extend the impedance control of manipulators carrying a heavy payload using an inner/outer loop control scheme in order to enhance the system robustness with respect to the robot dynamics uncertainties. We also assume that the desired impedance model relating the force and motion takes the following general form

$$\boldsymbol{M}_d(\boldsymbol{x})\ddot{\boldsymbol{x}} + \boldsymbol{h}_d(\dot{\boldsymbol{x}}, \boldsymbol{x}) = \boldsymbol{f}_{\text{ext}}. \qquad (13)$$

Here, we will assume without loss of generality that $\boldsymbol{x}_d \equiv \mathbf{0}$. It is worthwhile mentioning that an interesting application of such a impedance control approach is in zero-g emulation of a scaled spacecraft prototype under the test in a 1-g laboratory environment [19].

Let us define an estimation of the acceleration $\ddot{\boldsymbol{x}}^\star$ that is obtained by subtracting (2) from (13), i.e.,

$$\boldsymbol{M}_\triangle\ddot{\boldsymbol{x}}^\star + \boldsymbol{h}_\triangle = \boldsymbol{f}_s, \qquad (14a)$$

where

$$\boldsymbol{M}_\triangle \triangleq \boldsymbol{M}_d - \boldsymbol{M}_p \quad \text{and} \quad \boldsymbol{h}_\triangle \triangleq \boldsymbol{h}_d - \boldsymbol{h}_p.$$

It should be pointed out that variable $\ddot{\boldsymbol{x}}^\star$ does not have any physical meaning, rather it is just a definition. As will be shown later in this section, the manipulator establishes the desired impedance (13) if the actual acceleration $\ddot{\boldsymbol{x}}$ follows $\ddot{\boldsymbol{x}}^\star$.

Remark 1: By inspection, one can show that if condition (11) is satisfied, then matrix $\boldsymbol{M}_\triangle$ is invertible
Therefore, if (11) is satisfied, then the estimated velocity $\dot{\boldsymbol{x}}^\star$ can be obtained through a numerical integration of (14a), i.e.,

$$\dot{\boldsymbol{x}}^\star(t) = \int_0^t \boldsymbol{M}_\triangle^{-1}\big(\boldsymbol{f}_s - \boldsymbol{h}_\triangle\big)\mathrm{d}\tau, \qquad (14b)$$

and $\boldsymbol{x}^\star$ can be similarly obtained by another numerical integration. Note that $\ddot{\boldsymbol{x}}^\star$ and $\ddot{\boldsymbol{x}}$ are not necessarily equal and neither do their integrated values.

Now, the objective is to force the manipulator to follow the trajectory dictated by (14b). this goal can be achieved by using an inverse-dynamics controller [18], [20] based on the complete model (5a) and by compensating only for the external force $\boldsymbol{f}_{\text{ext}}$, which is not correlated to the inertial forces. However, the difficulty in this approach is that because of the acceleration estimation error, one can only obtain an estimation of the external force $\boldsymbol{f}_{\text{ext}}$; as will be show in the following analysis. Let

$$\ddot{\tilde{\boldsymbol{x}}} \triangleq \ddot{\boldsymbol{x}}^\star - \ddot{\boldsymbol{x}} \qquad (15)$$

denotes the acceleration error. Now, upon substitution of $\ddot{\boldsymbol{x}}^\star$ from (14a) into (15) and then substituting the resultant acceleration term into (2), we can write the expression of the external force as:

$$\boldsymbol{f}_{ext} = \boldsymbol{f}_{\text{ext}}^\star + \tilde{\boldsymbol{f}}_{\text{ext}},$$

where

$$\boldsymbol{f}_{\text{ext}}^\star = \big(\mathbf{1} + \boldsymbol{M}_p\boldsymbol{M}_\triangle^{-1}\big)\boldsymbol{f}_s + \boldsymbol{h}_p - \boldsymbol{M}_p\boldsymbol{M}_\triangle^{-1}\boldsymbol{h}_\triangle \qquad (16)$$

is the estimation of the external force and

$$\tilde{\boldsymbol{f}}_{ext} = -\boldsymbol{M}_p\ddot{\tilde{\boldsymbol{x}}} \qquad (17)$$

is the force estimation error. Clearly, the force estimation error goes to zero if and only if the acceleration error does so.

Now, considering the force estimation (16) for compensating the force perturbation, we propose the following inner loop control

$$\begin{aligned}\boldsymbol{u} &= \boldsymbol{M}_t(\boldsymbol{q})\ddot{\boldsymbol{x}}^\star + \boldsymbol{h}_t - \boldsymbol{f}^\star_{\rm ext} \\ &\quad + \boldsymbol{M}_t(\boldsymbol{q})\big(\boldsymbol{G}_d(\dot{\boldsymbol{x}}^\star - \dot{\boldsymbol{x}}) + \boldsymbol{G}_p(\boldsymbol{x}^\star - \boldsymbol{x})\big), \qquad (18)\end{aligned}$$

where $\ddot{\boldsymbol{x}}^\star$, $\dot{\boldsymbol{x}}^\star$, $\boldsymbol{x}^\star$ and $\boldsymbol{f}^\star_{\rm ext}$ are obtained from (13)- (16), while $\boldsymbol{G}_d > 0$ and $\boldsymbol{G}_p > 0$ are the feedback gains. In the following analysis, we will show that the inner loop controller (18) in conjunction with the outer loop (14) can shape the impedance of the combined system of manipulator and payload according to (13) provided that a condition on the system mass distribution is met. Substitution (18) into the dynamics model (5a) yields the equation of force error as

$$\boldsymbol{M}_t\big(\ddot{\tilde{\boldsymbol{x}}} + \boldsymbol{G}_d\dot{\tilde{\boldsymbol{x}}} + \boldsymbol{G}_p\tilde{\boldsymbol{x}}\big) = -\tilde{\boldsymbol{f}}_{\rm ext}. \qquad (19)$$

Using (17) in (19) yields the following autonomous system

$$\big(\boldsymbol{1} - \boldsymbol{M}_t^{-1}\boldsymbol{M}_p\big)\ddot{\tilde{\boldsymbol{x}}} + \boldsymbol{G}_d\dot{\tilde{\boldsymbol{x}}} + \boldsymbol{G}_p\tilde{\boldsymbol{x}} = \boldsymbol{0},$$

which is equivalent to

$$\begin{aligned}&\big(\boldsymbol{1} - \boldsymbol{M}_t^{-1}\boldsymbol{M}_p\big)\big(\ddot{\tilde{\boldsymbol{x}}} + \boldsymbol{G}_d\dot{\tilde{\boldsymbol{x}}} + \boldsymbol{G}_p\tilde{\boldsymbol{x}}\big) \\ &+ \boldsymbol{M}_t^{-1}\boldsymbol{M}_p\big(\boldsymbol{G}_d\dot{\tilde{\boldsymbol{x}}} + \boldsymbol{G}_p\tilde{\boldsymbol{x}}\big) = \boldsymbol{0}. \qquad (20)\end{aligned}$$

Multiplying both sides of (20) by $\boldsymbol{M}_m^{-1}\boldsymbol{M}_t$ and using identity (5b) in the resultant equations yields

$$\ddot{\tilde{\boldsymbol{x}}} + \boldsymbol{G}_d\dot{\tilde{\boldsymbol{x}}} + \boldsymbol{G}_p\tilde{\boldsymbol{x}} + \boldsymbol{\Delta}_m\big(\boldsymbol{G}_d\dot{\tilde{\boldsymbol{x}}} + \boldsymbol{G}_p\tilde{\boldsymbol{x}}\big) = \boldsymbol{0}, \qquad (21)$$

where

$$\boldsymbol{\Delta}_m \triangleq \boldsymbol{M}_m^{-1}\boldsymbol{M}_p. \qquad (22)$$

Stability of the closed-loop system (21) remains to be proved. We will show in the followings that system (21) remains stable if the coefficient matrix of the additive term, i.e., $\boldsymbol{\Delta}_m$, is sufficiently small. Let us assume that $\boldsymbol{z} = {\rm col}(\tilde{\boldsymbol{x}}, \dot{\tilde{\boldsymbol{x}}})$ represents the state vector. Then, (21) can be written in the following compact form

$$\dot{\boldsymbol{z}} = \boldsymbol{A}\boldsymbol{z} + \boldsymbol{d}(t, \boldsymbol{z}), \qquad (23)$$

where

$$\boldsymbol{A} = \begin{bmatrix}\boldsymbol{0} & \boldsymbol{1} \\ -\boldsymbol{G}_p & -\boldsymbol{G}_d\end{bmatrix} \quad \text{and} \quad \boldsymbol{d}(t,\boldsymbol{z}) = -\boldsymbol{D}\boldsymbol{\Delta}_m\boldsymbol{G}\boldsymbol{z},$$

with $\boldsymbol{G} = [\boldsymbol{G}_p \quad \boldsymbol{G}_d]$ and $\boldsymbol{D}^T = [\boldsymbol{0} \quad \boldsymbol{1}]$. Since the perturbation term $\boldsymbol{d}$ satisfies the linear growth bound

$$\|\boldsymbol{d}\| \leq \|\boldsymbol{G}\|\|\boldsymbol{\Delta}_m\|\|\boldsymbol{z}\|,$$

where

$$\frac{\lambda_{\min}(\boldsymbol{M}_p)}{\lambda_{\max}(\boldsymbol{M}_m)} \leq \|\boldsymbol{\Delta}_m\| \leq \frac{\lambda_{\max}(\boldsymbol{M}_p)}{\lambda_{\min}(\boldsymbol{M}_m)} < \infty \qquad \forall \boldsymbol{z} \in \mathbb{R}^{2n},$$

system (23) is in the form of *vanishing perturbation* [21]—here, $\|\cdot\|$ denotes the Euclidean norm of a vector or a matrix. Moreover, since $\boldsymbol{A}$ is Hurwitz, one can show that the perturbed system can be globally exponentially stable if the gains are adequately selected, i.e.,

$$\|\boldsymbol{\Delta}_m\| \leq \kappa(\boldsymbol{G}), \qquad (24)$$

where $\kappa(\boldsymbol{G})$ is a function of the feedback gains; see the Appendix II for details. That means there must exist scalar $\mu > 0$ such that $\|\boldsymbol{z}\| \leq \|\boldsymbol{z}(0)\| e^{-\mu t}$. Therefore, it can be inferred from (21) that

$$\|\ddot{\tilde{\boldsymbol{x}}}\| \leq \phi e^{-\mu t}, \qquad (25)$$

where scaler ϕ depend on the initial error

$$\phi = (1 + \|\boldsymbol{\Delta}_m\|)\,\|\boldsymbol{G}\|\,\boldsymbol{z}(0).$$

Now, we are ready to derive the input/output relation of the closed loop system under the proposed control law. Adding both sides of (2) and (14a) yields

$$\boldsymbol{M}_d\ddot{\boldsymbol{x}} + \boldsymbol{h}_d(\dot{\boldsymbol{x}}, \boldsymbol{x}) = \boldsymbol{f}_{\rm ext} + \boldsymbol{\delta}, \qquad (26a)$$

where

$$\boldsymbol{\delta}(t) = -\boldsymbol{M}_\Delta\ddot{\tilde{\boldsymbol{x}}}. \qquad (26b)$$

It follows from (25) and (26b) that

$$\|\boldsymbol{\delta}\| \leq \phi\lambda_{\max}(\boldsymbol{M}_\Delta)e^{-\mu t}, \qquad (27)$$

which means that the perturbation $\boldsymbol{\delta}$ exponentially relaxes to zero from its initial value.

To summarize, consider the target impedance dynamics (13) for a manipulator with inertia $\boldsymbol{M}_m$ carrying a payload with $\boldsymbol{M}_p$. Assume that the inertia ratios $\|\boldsymbol{\Delta}_d\|$ and $\|\boldsymbol{\Delta}_m\|$ satisfy conditions (11) and (24), respectively. Then, the force-response of the combined manipulator and payload under the impedance controller with the inner/outer loops (14)-(18) converges to the target impedance (13), while the control input remains bounded.

TABLE I
MANIPULATOR'S LINK PARAMETERS.

Parameters	Link 1	Link 2	Link 3	Link 4	Link 5	Link 6
m (kg)	27.31	21.00	10.00	4.33	4.02	1.59
I_{xx} (kgm^2)	0.31	0.35	0.17	0.035	0.026	0.01
I_{yy} (kgm^2)	0.38	3.30	2.60	0.05	0.04	0.01
I_{zz} (kgm^2)	0.30	-0.490	2.50	0.02	0.02	0.003
c_x (m)	-0.140	-4.90	-0.401	-0.166	-0.162	0.000
c_y (m)	-0.044	0.000	0.000	0.079	-0.009	0.000
c_z (m)	0.170	0.125	0.030	0.171	0.204	0.220

IV. EXPERIMENT

This section describes experimental results obtained from implementation of the proposed impedance control scheme using a robotic manipulator at the robotics laboratory of the Canadian Space Agency (CSA), see Fig. 2. The inertial properties of the manipulator links have been identified [22] as listed in Table I. A dummy box which weights 16 kg, is mounted on the manipulator wrist. The payload inertia is calculated to be $\boldsymbol{I}_p = {\rm diag}(0.33,\ 0.62\ ,0.71)$ kgm^2. The target inertia of the impedance controller is set to be three times higher than the actual mass and inertia of the payload. The force/moment interaction between the manipulator and the payload were measured by a six-axis JR3 force/moment sensor. The impedance controller scheme (14)-(18) was developed using Simulink and matrix manipulation was performed by using the DSP Blockset of

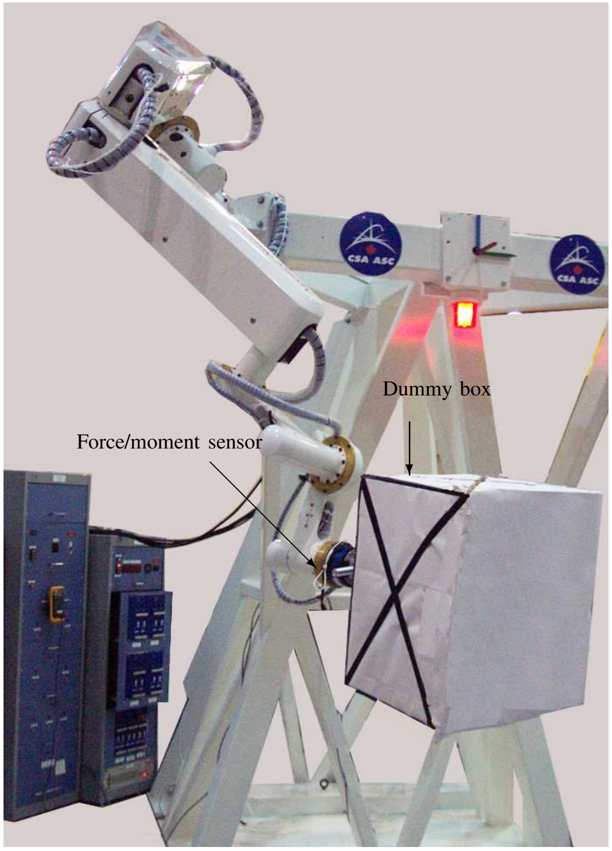

Fig. 2. The manipulator carrying a payload.

Matlab/Simulink [23]. The Real-Time Workshop package [24] generated portable C code from the Simulink model which was executed on a QNX real-time operating system.

The objective of the experiment is to show that the proposed controller is able to match the manipulator force-response according to the desired impedance even though the force sensor signal is directed incorporated into the controller without compensating for the inertial forces. Fig. 3 shows trajectories of the forces and moments due to external force impulses applied by hand. Note that despite the fact that the external forces and moments can not be directly measured, they can be estimated by making use of the dynamics model of the load. The subsequent trajectories of the linear and angular velocities of the payload are illustrated in Fig. 4(a). The simulated velocity profiles according to the target impedance model are also depicted in Fig. 4(b). A comparison between trajectories of Figs. 4(a) and 4(b) shows that the impedance controller has succeeded to establish the target impedance characteristic even though the wrist force sensor sees inertial forces of the load.

V. Conclusions

An impedance controller for manipulators carrying a rigid-body payload has been developed that does not rely on any acceleration measurements in order to compensate for the inertial forces of the payload. The stability and convergence of the impedance controller have been ana-

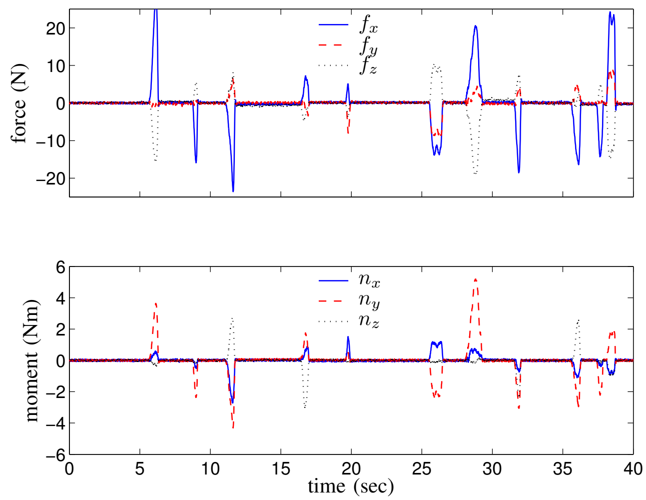

Fig. 3. Dynamics force and moment.

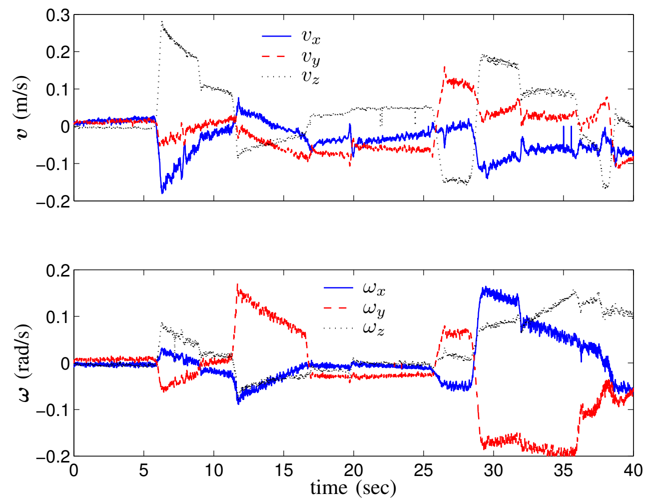

(a) Actual trajectories

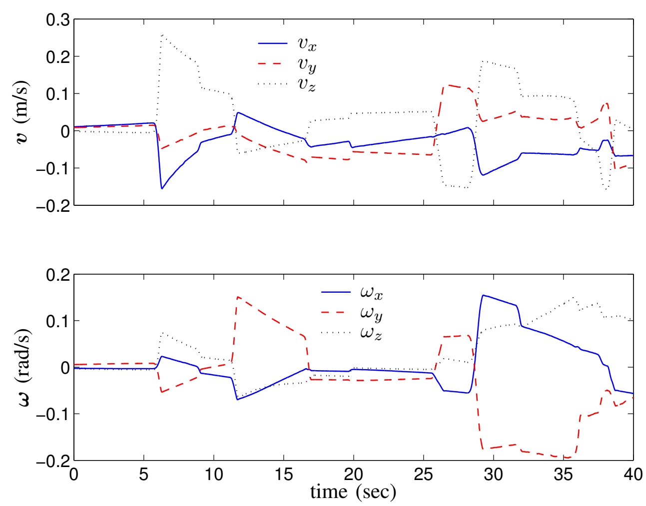

(b) Simulated trajectories

Fig. 4. Trajectories of the linear and angular velocities.

lytically investigated. The results showed that the control input remains bounded provided that the desired inertia was selected to be different from that of the payload. The impedance controller was further developed with utilizing an inner/outer loop approach. This allows specifying the desired impedance model in a general form. Moreover, the robust control theory was employed to modify the proposed impedance controller so that it could compensate for robot modeling uncertainty. Experimental results have shown that the proposed impedance controller enabled a manipulator carrying a payload with a non-negligible mass to establish the desired impedance characteristic even though no acceleration measurements were used.

APPENDIX I

Dynamics equations of the manipulator in the joint space is described by

$$\boldsymbol{M}'_m\ddot{\boldsymbol{q}} + \boldsymbol{h}'_m(\boldsymbol{q},\dot{\boldsymbol{q}}) = \boldsymbol{\tau} + \boldsymbol{J}^T\boldsymbol{f}_s \tag{28}$$

Substituting the joint acceleration from $\ddot{\boldsymbol{q}} = \boldsymbol{J}^{-1}\ddot{\boldsymbol{x}} - \boldsymbol{J}^{-1}\dot{\boldsymbol{J}}\dot{\boldsymbol{q}}$ into (28) and then multiply the resultant equation by $\boldsymbol{J}^{-T}$ yields (4), in which

$$\boldsymbol{M}_m \triangleq \boldsymbol{J}^{-T}\boldsymbol{M}'_m\boldsymbol{J}^{-1}$$
$$\boldsymbol{h}_m \triangleq \boldsymbol{J}^{-T}\boldsymbol{h}'_m - \boldsymbol{M}_m\dot{\boldsymbol{J}}\dot{\boldsymbol{q}}$$

APPENDIX II

Since $\boldsymbol{A}$ is Hurwitz, there exists Lyapunov function

$$V(\boldsymbol{z}) = \boldsymbol{z}^T\boldsymbol{P}\boldsymbol{z} \tag{29}$$

with $\boldsymbol{P} > 0$ satisfying

$$\boldsymbol{P}\boldsymbol{A} + \boldsymbol{A}^T\boldsymbol{P} = -\boldsymbol{1}. \tag{30}$$

The derivative of $V(\boldsymbol{z})$ along trajectories of perturbed system (23) satisfies

$$\dot{V} \leq \Big(-1 + 2\,\|\boldsymbol{G}\|\,\lambda_{\max}(\boldsymbol{P})\,\|\boldsymbol{\Delta}_m\|\Big)\,\|\boldsymbol{z}\|^2. \tag{31}$$

Therefore, according to the stability theorem of perturbed system [21, p. 206], the origin of (23) is globally exponentially stable if

$$\|\boldsymbol{\Delta}_m\| \leq \kappa(\boldsymbol{G}_p,\boldsymbol{G}_d) \triangleq \frac{1}{2\,\|\boldsymbol{G}\|\,\lambda_{\max}(\boldsymbol{P})}. \tag{32}$$

REFERENCES

[1] N. Hogan, "Impedance control an approach to manipulation: Part i - theory," *Journal of Dynamic Systems, Measurement, and Control*, vol. 107, pp. 1–7, 1985.

[2] ——, "Stabel execution of contact tasks using impedance control," in *IEEE Int. Conf. on Robotcis & Automation*, Raleigh, North Carolina, USA, April 1987, pp. 1047–1054.

[3] E. Colgate and N. Hogan, "An analysis of contact stability in terms of passive physical equivalents," in *IEEE Int. Conf. on Robotcis & Automation*, Scottsdale, Arizona, USA, Mayl 1989, pp. 404–409.

[4] T. Lasky and T. C. Hsia, "On force-tracking impedance control of robot manipulator," in *IEEE Int. Conf. on Robotcis & Automation*, Sacramento, USA, April 1991, pp. 274–280.

[5] W.-S. Lu and Q.-H. Meng, "Impedance control with adaptation for robotic manipulators," *IEEE Trans. on Robotics & Automation*, vol. 7, no. 2, pp. 408–415, 1991.

[6] R. Carelli and R. Kelly, "An adaptive impedance/force controller for robot manipulators," *IEEE Trans. on Automatic Control*, vol. 36, no. 8, pp. 967–971, August 1991.

[7] S. Lee and H. S. Lee, "Intelligent control of manipulators interfacing with anuncertain environment based on generalized impedance," in *IEEE Symp. Intelligent Control*, 1991, pp. 61–66.

[8] F. Aghili and M. Namvar, "A robust impedance matching scheme for emulation of robots," in *IEEE/RSJ Int. Conf. on Intelligent Robots and Systems*, Sendai, Japan, September 28–October 2 2004, pp. 2142–2148.

[9] S. Jung, T. C. Hsia, and R. G. Bonitz, "Force tracking impedance control of robot manipulators under unknown environment," *IEEE Trans. on Control Systems Technology*, vol. 12, no. 3, pp. 474–483, May 2004.

[10] O. Khatib, "A unified approach for motion and force control of robot manipulators: The operational space formulation," *IEEE Transactions on Robotics and Automation*, vol. RA-3, no. 1, pp. 43–53, 1987.

[11] M. Fujita and H. Inoue, "A study on processing of force sensor signals," in *1 st. Anual Conf. of The Robotics Society of Japan*, Tokyo, 1979, pp. 153–160.

[12] M. Uchiyama and K. Kitagaki, "Dynamics force sensing for high-speed robot manipulation using kalman filtering techniques," in *IEEE Int. Conf. Decision and Control*, Tampa, FL, December 1989, pp. 2147–4152.

[13] D. Kubus, T. Kroger, and F. M. Wahl, "On-line rigid object recognition and pose estimation based on inertial parameters," in *IEEE/RSJ Int. Conference on Intelligent Robots and Systems*, San Diego, CA, Oct. 29–Nov. 2 2007, pp. 1402–1408.

[14] ——, "Improving force control performance by computational elimination of non-contact force/torque," in *IEEE International Conference on Robotics & Automation*, Pasadena, CA, May 2008, pp. 2617–2622.

[15] J. Garcia, A. Robertsson, J. G. Ortega, and R. Johansson, "Generalized contact force estimator for a robot manipulator," in *IEEE Int. Conf. on Robotics & Automation*, Orlando, FL, May 2006, pp. 4019–4024.

[16] Letitmann, "On the efficacy of nonlinear control in uncertain linear systems," *ASME Journal of Dynamics Systems, Measurement, and Control*, vol. 102, no. 2, pp. 95–102, 1981.

[17] M. W. Spong and M. Vidyasagar, *Robot Dynamics and Control*. New York, NY: Wiley, 1989, pp. 224–236.

[18] C. Canudas de Wit, B. Siciliano, and G. Bastin, Eds., *Theory of Robot Control*. London, Great Britain: Springer, 1996.

[19] F. Aghili, M. Namvar, and G. Vukovich, "Satellite simulator with a hydraulic manipulator," in *IEEE Int. Conference on Robotics & Automation*, Orlando, Florida, May 2006, pp. 3886–3892.

[20] M. W. Spong and M. Vidyasagar, *Robot Dynamics and Control*. New York, NY: Wiley, 1989.

[21] H. K. Khalil, *Nonlinear Systems*. New-York: Macmillan Publishing Company, 1992.

[22] T. Lamarche, "CSA Automation and Robotics Testbed: Dynamics model," Canadian Space Agency, Tech. Rep. CSA-ST-CART-2002-002, 2002.

[23] *DSP Blockset for Use with Simulink, User's Guide*, The MathWorks Inc., 24 Prime Parlway, Natick, MA 011760-1500, 1998.

[24] *Real-Time Workshop for Use with Simulink*, 5th ed., The MathWorks Inc., 3 Apple Hill Drive, Natick, MA 011760-2098, 2002.